LCAT cholesterol esterification is associated with the increase of ApoE/ApoA-I ratio during atherosclerosis progression in rabbit

Alessandro Carlucci, Luisa Cigliano, Bernardetta Maresca, Maria Stefania Spagnuolo, Giovanni Di Salvo, Raffaele Calabrò, et al.

Journal of Physiology and Biochemistry
Official Journal of the University of Navarra, Spain

ISSN 1138-7548
Volume 68
Number 4

J Physiol Biochem (2012) 68:541-553
DOI 10.1007/s13105-012-0172-0

Springer

J Physiol Biochem (2012) 68:541–553
DOI 10.1007/s13105-012-0172-0

ORIGINAL PAPER

LCAT cholesterol esterification is associated with the increase of ApoE/ApoA-I ratio during atherosclerosis progression in rabbit

Alessandro Carlucci · Luisa Cigliano · Bernardetta Maresca · Maria Stefania Spagnuolo · Giovanni Di Salvo · Raffaele Calabrò · Paolo Abrescia

Received: 13 October 2011 / Accepted: 11 April 2012 / Published online: 5 May 2012

Abstract Apolipoprotein A-I and Apolipoprotein E promote different steps of reverse cholesterol transport, including lecithin-cholesterol acyltransferase stimulation. Our aim was to study the changes in the levels of Apolipoprotein A-I, Apolipoprotein E, and lecithin-cholesterol acyltransferase activity during atherosclerosis progression in rabbits. Quantitative echocardiographic parameters were analyzed in order to evaluate, for the first time, whether atherosclerosis progression in rabbit is associated to apolipoproteins changes and alteration of indices of cardiac function, such as systolic strain and strain rate of the left ventricle. Atherosclerosis was induced by feeding rabbits for 8 weeks with 2 % cholesterol diet. The HDL levels of cholesterol and cholesteryl esters were measured by HPLC. The lecithin-cholesterol acyltransferase activity was evaluated both ex vivo, as cholesteryl esters/cholesterol molar ratio, and in vitro. Apolipoproteins levels were analyzed by ELISA. The HDL levels of cholesterol and cholesteryl esters increased, during treatment, up to 3.7- and 2.5-fold, respectively, compared to control animals. The lecithin-cholesterol acyltransferase activity in vitro was halved after 4 weeks. During cholesterol treatment, Apolipoprotein A-I level significantly decreased, whereas Apolipoprotein E concentration markedly increased. The molar ratio Apolipoprotein E/Apolipoprotein A-I was negatively correlated with the enzyme activity, and positively correlated with both increases in the intima-media thickness of common carotid wall and cardiac dysfunction signs, such as systolic strain and strain rate of the left ventricle.

Keywords Atherosclerosis · Rabbit · Cholesterol · Apolipoprotein A-I · Apolipoprotein E · Lecithin cholesterol acyltransferase

Alessandro Carlucci and Luisa Cigliano contributed equally to this study.

Further studies on humans or other animal models could be of help to confirm whether the ratio Apolipoprotein E/Apolipoprotein A-I can be considered as a biomarker of atherosclerosis progression.

A. Carlucci · L. Cigliano (✉) · B. Maresca · P. Abrescia
Dipartimento delle Scienze Biologiche-Sezione di Fisiologia ed Igiene, Università di Napoli Federico II, via Mezzocannone 8, 80134 Naples, Italy
e-mail: luisa.cigliano@unina.it

M. S. Spagnuolo
Istituto per il Sistema Produzione Animale in Ambiente Mediterraneo, Consiglio Nazionale delle Ricerche, Naples, Italy

G. Di Salvo · R. Calabrò
Dipartimento di Cardiologia, Divisione di Cardiologia Pediatrica, Seconda Università di Napoli, Ospedale Monaldi, Naples, Italy

Introduction

The HDL apolipoproteins ApoA-I and ApoE impair the onset and progression of atherosclerosis by playing

a pivotal role in a multi-step process called "reverse cholesterol transport" (RCT) [13, 17, 19]. In particular, Apolipoprotein A-I (ApoA-I) and Apolipoprotein E (ApoE) promote the efflux of cholesterol excess from cells [19], and stimulate lecithin cholesterol acyltransferase (LCAT) to convert free cholesterol into cholesteryl esters, which are embedded into the lipoprotein core, and change particle shape and density [4, 11, 42]. Spherical lipoproteins are thus formed and mostly contribute to the heterogeneous population of circulating HDL [19]. Finally, ApoA-I and ApoE act as HDL ligands for hepatocyte receptors and deliver their lipid cargo, including free cholesterol and cholesteryl esters, to liver for elimination [17, 19]. Plasma levels of large or small HDL subfractions were reported to be associated with the progression of coronary atherosclerosis [8, 27].

Rabbits share with humans most HDL-remodelling enzymes and, when fed a high cholesterol diet, rapidly develop severe hypercholesterolemia leading to atherosclerosis [14, 40]. They have been used as animal model to study potential predictors of atherosclerosis development or therapies against the progression of the disease [40]. We focused on cholesterol-fed rabbits because they represent an ideal animal model to create extreme conditions of cholesterol excess and study consequent alteration of critical players of RCT, i.e., LCAT, ApoA-I, and ApoE.

A major problem is the lack of sensitive and objective plasma markers for early diagnosis of individuals at risk of coronary heart disease and/or to follow the progression of the disease. The aim of this study was to analyse, in cholesterol fed rabbits, the changes in the levels of ApoA-I, ApoE, and LCAT activity during atherosclerosis progression. Furthermore, this study sought to determine whether cholesterol treatment induces alteration of both intima-media thickness and indices of cardiac function. The correlation of these parameters with changes of apolipoproteins or LCAT activity was also explored.

Materials and methods

Materials

RAM11 (mouse monoclonal antibody anti-rabbit macrophage) was purchased from Santa Cruz [Santa Cruz, California, USA]. Goat anti-ApoE polyclonal antibody was purchased from Chemicon [Millipore, Billerica, MA, USA]. Human ApoE was obtained from Calbiochem [La Jolla, CA, USA]. Sheep anti-ApoA-I purchased from Serotec [Oxford, UK]. [1α,2α-^{3}H]Cholesterol (45 Ci/mmol) was obtained from Perkin Elmer [Boston, MA, USA]. Sil-G plates for Thin Layer Chromatografy (TLC; thickness 0.25 mm) were obtained from Macherey-Nagel [Düren, Germany]. Chemicals of the highest purity, thyroglobulin, ferritin, lactate dehydrogenase, bovine serum albumin (BSA) cholesterol, egg yolk lecithin, rabbit anti-goat HRP-conjugated (RAG-HRP) IgG, donkey anti-sheep HRP-conjugated (DAS-HRP) IgG, goat anti-mouse HRP-conjugated peroxidase (GAM-HRP) IgG, *o*-phenylenediamine, dextran sulphate (DS, 50 kD), 4-chloro-1-naphtol, molecular weight markers, Supelcosil LC-18 (5 μm particle size, 250× 4.6 mm I.D.) were obtained from Sigma-Aldrich [St Louis, MO, USA]. Ketamine, Acepromazine, Diazepam, and Tanax were obtained from Alcyon [Marene, CN, Italy]. LDL-cholesterol direct colorimetric kit was obtained from PKL, Pokler [Salerno, Italia]. PVDF transfer membrane of Millipore [Bedford, MA, USA] was used. Organic solvents were purchased from Romil [Cambridge, UK]. Polystyrene 96 wells plates were purchased from Nunc [Roskilde, Denmark].

Methods

Rabbits' treatment

Male New Zealand white rabbits weighing 1.4–1.6 kg (Harlan, Correzzana (MI), Italy) were fed for 8 weeks with Purina® standard feed as such (control group) or containing 2 % (*w*/*w*) cholesterol (treated group). Both feeds were purchased from Cargill (Milano, Italia). During treatment, blood samples were collected from the marginal ear vein. Plasma was separated by centrifugation at 800×*g* for 15 min at 4°C. During the echocardiographic analysis, the rabbits were anesthetized with intravenous injection of Ketamine (25 mg/Kg), Acepromazine (1 mg kg^{-1}), and Diazepam (2 mg kg^{-1}). After 8 weeks, the rabbits were anesthetized and then sacrificed by administration of Tanax (0.3 ml kg^{-1}). The aortic arch of each rabbit was dissected free of adhering tissue, washed with physiological solution, and perfusion-fixed with Bouin's fluid for 18 h [10]. The specimens were then dehydrated through a graded ethanol series, soaked in

paraffin, and serially and transversally cut for histochemistry. Standard principles of laboratory animal care were in accordance with accepted institutional policies, and all procedures were approved by the Animal Ethics Committee of the University of Naples Federico II.

Histochemistry

Tissue cross-sections (5 μm thick) were prepared from aortic arch. Some of them were stained with Azan-Mallory trichrome method according to a published procedure [10]. Other sections were processed for histochemistry using a monoclonal antibody (RAM11) against the macrophage marker CD68. In detail, deparaffinized and hydrated sections were washed in PBS (50 mM Na_2HPO_4/NaH_2PO_4, pH 7.4) for 10 min, treated with 0.3 % hydrogen peroxide for 30 min, incubated with 0.5 % BSA for 30 min, and finally challenged with RAM11 (dilution 1:100 in PBS containing 0.25 % BSA) at 4°C over night. After washing by PBS, the sections were incubated with GAM-HRP (dilution 1:100 in PBS containing 0.25 % BSA) for 60 min, washed again by PBS, incubated with 0.1 % diaminobenzidine tetrahydrocloride and 0.3 % H_2O_2 in PBS, and finally counterstained with Mayer's hematoxylin and mounted for light microscopy. Negative controls were prepared by omitting the incubation with the primary antibody. Images of the treated sections were acquired by a software-assisted camera system (KS300 from Zeiss, Zaventem, Belgium).

ELISA

Plasma concentrations of ApoA-I and ApoE were titrated by ELISA. Rabbit ApoA-I, isolated according to a published procedure [3] and exhibiting over 98 % purity by electrophoresis and densitometric analysis, was used for calibration. The level of ApoE was determined by using the human antigen as standard for calibration. The ApoA-I and ApoE levels were determined both in the whole plasma and in the supernatant obtained after precipitation of plasma LDL and VLDL with 0.1 % DS in 50 mM $MnCl_2$ (DS-treated plasma). Aliquots of plasma or DS-treated plasma (50 μL from 1:1,000, 1:10,000, 1:20,000, 1:45,000, 1:60,000, and 1:100,000 dilutions in 7.3 mM Na_2CO_3, 17 mM $NaHCO_3$, 1.5 mM NaN_3, pH 9.6), were loaded into the wells of a microtiter plate, and processed essentially according to a published procedure [6]. In particular, sheep or goat IgG (anti-ApoA-I, 1:1,500 dilution, or anti-ApoE, 1:2,000 dilution, respectively) was used as primary antibody, and DAS-HRP IgG or RAG-HRP IgG (1:3,000 dilution and 1: 8,000 dilution, respectively) as secondary antibody for color development.

LCAT activity assay

Plasma samples from cholesterol-fed and control animals were treated with 0.1 % DS in 50 mM $MnCl_2$ to remove VLDL and LDL [6]. The in vitro activity of LCAT was measured as described previously [5, 32], using a proteoliposome (ApoA-I: lecithin: cholesterol=1.5:200:18 molar contribution; 0.7 μM ApoA-I in the assay) as substrate. The enzyme activity was expressed as nanomole of cholesterol esterified per hour per milliliter of plasma (units). The efficiency of LCAT stimulation by ApoA-I or ApoE was investigated by incubating a pool of DS-treated plasma, obtained from control rabbits (as enzyme source) with proteoliposomes containing different molar ratios of ApoA-I with ApoE (4:0, 3:1, 2:2, 1:3, or 0:4; 0.4 μM apolipoprotein in the assay) as substrate.

Titration of cholesterol and cholesteryl esters in HDL

Plasma samples of cholesterol-fed or control animals were treated with 0.1 % DS in 50 mM $MnCl_2$ for removing VLDL and LDL [6]. The absence of VLDL and LDL in DS-treated plasma was verified by enzymatic colorimetric method [1], using a commercial kit, according to the manufacturer's instructions. After this treatment, two aliquots of DS-treated plasma (25 μL) were used for measuring the amount of free cholesterol (FC) and total cholesterol. In detail, one aliquot was incubated with 0.25 mL of ethanol, while the other one with 0.25 mL of ethanol containing 5 M KOH. After incubation (1 h, 75°C), both mixtures were supplemented with 0.15 mL of 1 % NaCl and, after addition of 2 mL of ice-cold hexane, were vigorously shaken for 2 min. Each hexane extract was taken on and the lower phase was likewise extracted two more times. The three extracts were pooled and dried under nitrogen stream. The residue was dissolved in 0.2 mL of acetonitrile/isopropanol (57:43, *v*:*v*), and 20 μL were processed by reverse-phase HPLC. The chromatography was

performed by a C18 column at 40°C with 1 mL min^{-1} flow rate, according to a published procedure [6]. The amounts of free and total cholesterol, as measured in the samples processed without and with KOH, respectively, were used to calculate the amount of cholesteryl esters (CE) as "total minus free cholesterol". Calibration curves ($r^2 \geq 0.9997$), obtained by injecting different amounts ($n=12$) of standard FC, were used for quantitative analysis.

Electrophoresis and densitometry

In order to check whether DS-treated plasma was contaminated by ApoB-containing lipoproteins, pools of whole plasma ($N=5$) and DS-treated plasma from cholesterol-fed (after 8 weeks of diet) and control rabbits were analyzed by electrophoresis. Proteins were fractionated by 3–10 % (*w*/*v*) polyacrylamide gradient gel electrophoresis, under denaturing and reducing conditions, and then blotted onto PVDF membrane [5]. After protein blotting, the membrane was rinsed in TBS (130 mM NaCl, 20 mM Tris–HCl, pH 7.4) containing 0.05 % (*v*/*v*) Tween 20 (T-TBS), and treated with 0.5 % BSA in TBS for 1 h at 37°C. ApoB presence was analyzed by incubating the membrane with goat anti-ApoB IgG (1:1,000 dilution in TBS containing 0.25 % BSA; 1 h at 37°C), followed by RAG-HRP IgG (1:3,000 dilution; 1 h at 37°C). The immune complexes were detected by using hydrogen peroxide and 4-chloro-1-naphthol for color development. ApoB was detected only in whole plasma, but not in DS-treated plasma, confirming that all ApoB containing lipoproteins were precipitated by DS treatment (data not shown).

The separation of HDL population in subfractions was performed as follows. Aliquots (2 μL) of a pool of DS-treated plasma obtained from cholesterol fed and control rabbits were processed for electrophoresis on 4–30 % (*w*/*v*) polyacrylamide gradient gel [18]. Homogeneity and hydrodynamic diameter of HDL were estimated using reference globular proteins (thyroglobulin, ferritin, lactate dehydrogenase, and albumin; Stokes' diameter, 17, 12.2, 8.1, and 7.1, respectively) [18]. After electrophoresis, proteins were blotted onto PVDF membrane. The membrane was treated with 5 % non fat milk in T-TBS (1 h, 37°C), and then incubated, overnight at 4°C, with sheep anti-ApoA-I or goat anti-ApoE IgG (1:1,000 dilution in T-TBS containing 0.25 % non fat milk). The immunocomplexes were detected by DAS-HRP or GAR-HRP IgG, respectively (1:1,000 dilution in T-TBS containing 0.25 % non fat milk), using hydrogen peroxide and 4-chloro-1-naphthol for color development. Digital images of membranes were analyzed by densitometry with the Gel-Pro Analyser software (Media Cybernetics, Silver Spring, MA). The band intensities were recorded as peaks on a densitogram and arbitrarily expressed as Integrated Optical Density (IOD).

Echocardiography

Echocardiographic studies were performed at baseline, 4, and 8 weeks of cholesterol treatment. Two-dimensional targeted M-mode traces were obtained at the level of the papillary muscles using an echocardiographic system equipped with a 10-MHz phased-array transducer. Anterior and posterior end-diastolic wall thickness, left ventricular (LV) contractility end-diastolic, and end-systolic dimensions were measured, according to the American Society for Echocardiography leading-edge method [31], from at least three consecutive cardiac cycles. LV volume and ejection fraction were calculated on the basis of the Teichholtz formula [34]. Data were collected by the Aplio XG echo-scanner and the Toshiba PSM-70AT transducer (5–10 MHz) with high temporal and spatial resolution. The transducer was placed directly on the chest wall and fixed at the parasternal view and then at the apical 4 chamber view (for color Doppler myocardial imaging, CDMI) using a mechanical arm. Using a zoomed image window, myocardial velocity data were acquired at rate of 203 frames s^{-1}, a sector angle of 30°, and an image depth of 15 mm. Beam focus was set at 10 mm. Digital data of ten consecutive heart cycles were recorded and transferred to a personal computer workstation for off-line analysis. Longitudinal myocardial velocities, systolic strain (S), and strain rate (SR) of the left ventricle were calculated from CDMI data using the Toshiba software. SR and S profiles were analyzed on the basal part of the interventricular septum. The region of interest was placed in the wall always in order to reduce the angle between the ultrasound beam and the muscle. S estimation length of 1.0 mm was used depending on the thickness of the wall (end-diastolic wall thickness between 1.1 and 2 mm). Start and end of the ejection phase were properly defined using ECG and velocity trace, as previously demonstrated in humans [33]. SR and S profiles were handled without smoothing. Peak systolic SR and S values were measured in each of ten heart cycles. The maximal and minimal values were

discarded, and the remaining eight values were averaged. The serial changes of peak systolic SR and S, before and during treatment, were then evaluated. All the echocardiographic analyses were performed on digitally stored raw data (gray scale bidimensional images and CDM images) by two investigators blinded to the treatment group and to the histological findings.

Statistical analysis

The samples for measurement of apolipoprotein concentration and LCAT activity were processed in triplicate. Echocardiographic data were also collected in triplicate. Data were expressed as means±standard deviation (SD). Statistical differences were determined using *t* test or, where appropriate, one-way ANOVA, followed by Tukey's test for multiple comparisons (GraphPad Software Inc., San Diego, CA). Differences were considered statistically significant when the two-sided *P* value was less than 0.05.

Results

Influence of cholesterol diet on lesion formation

Histological analysis of the aortic arch was performed to assess the presence of atherosclerotic plaques. The sections were obtained from rabbits fed standard diet or high cholesterol diet for 8 weeks. The intima was barely visible and no plaque was detected, after Azan-Mallory staining, in aorta sections from control group (Fig. 1a). In the cholesterol-treated group, the intima/media ratio was approximately twofold greater than that in control group, and atherosclerotic plaques were detected (Fig. 1c). In particular, these plaques contained a large amount of thick fatty streaks with round lipid-loaded cells, which turned out to be macrophages as detected by anti-RAM11 antibodies (Fig. 1d vs. b). The macrophages clearly displayed penetration into the media layer.

Ratio of CE with FC in HDL of normal or cholesterol-fed rabbits

The activity of LCAT was evaluated in rabbit plasma by measuring the amount of CE and FC in HDL. In particular, the molar ratio of CE with FC in HDL, a parameter used to evaluate the enzyme activity ex vivo [6], was calculated. Plasma samples were collected from cholesterol-fed (N=5) or control rabbits (N=5), and analyzed at different time lengths. The CE level was found markedly higher in cholesterol fed rabbits than in controls, starting from the fourth week of treatment (4 weeks, 2.38±0.36 vs. 1.2±0.1 mM, $P<0.01$; 6 weeks, 2.6±0.24 vs. 1.3±0.1 mM, $P<0.01$; 8 weeks, 2.9±0.42 vs. 1.1±0.15 mM, $P<0.01$) (Fig. 2a). As expected, the HDL FC level was higher in cholesterol-fed rabbits than in controls (Fig. 2a), from the fourth week of treatment (4 weeks, 0.72±0.22 vs. 0.20±0.03 mM in controls, $P<0.01$) and from then onwards (6 weeks, 0.8±0.1 vs. 0.25±0.05 mM, $P<0.01$; 8 weeks, 0.86±0.25 vs. 0.23±0.04 mM, $P<0.01$). It is worth to note that the level of HDL-FC increased more than that of HDL-CE during treatment (about 3.8- and 2-fold, respectively). The CE/FC ratio did not change after 1 week of treatment, whereas it decreased afterwards as a logarithmic function of time length (r=0.9522), thus indicating that the HDL composition in FC and CE was not immediately modified by the cholesterol loading but only a few days later. The ratio progressively and significantly decreased from the second to the third week of treatment (down to 53±10 % of the value at the starting point), and poorly changed ever since (8 weeks, 50±12 %) (Fig. 2b). In particular, after 2 weeks of treatment, the CE/FC ratio was significantly lower (30 % lower of initial value) than that in controls. The control group did not display significant alterations of CE/FC ratio. In agreement with these data, the amount of plasma LCAT, when measured in vitro by determining the enzyme activity after 4 weeks of treatment, was found to be about half of that in control rabbits (3.3±0.8 vs. 7.8±0.6 units, $P<0.01$), and no further significant decrease until the end of treatment was observed (3.9±0.9 vs. 8.1±0.7 units, $P<0.01$) (Fig. 3).

ApoA-I and ApoE levels in normal or cholesterol-fed rabbits

The major LCAT stimulating effectors are ApoA-I and ApoE [4, 11, 42]. Therefore, in order to get more insight into the regulation of enzyme activity, it was mandatory to analyze the levels of these two apolipoproteins during the dietary treatment. Plasma from rabbits, fed with normal or cholesterol diet, was collected at different times (0, 2, 4, 6, and 8 weeks) and treated with DS to remove VLDL and LDL. Then,

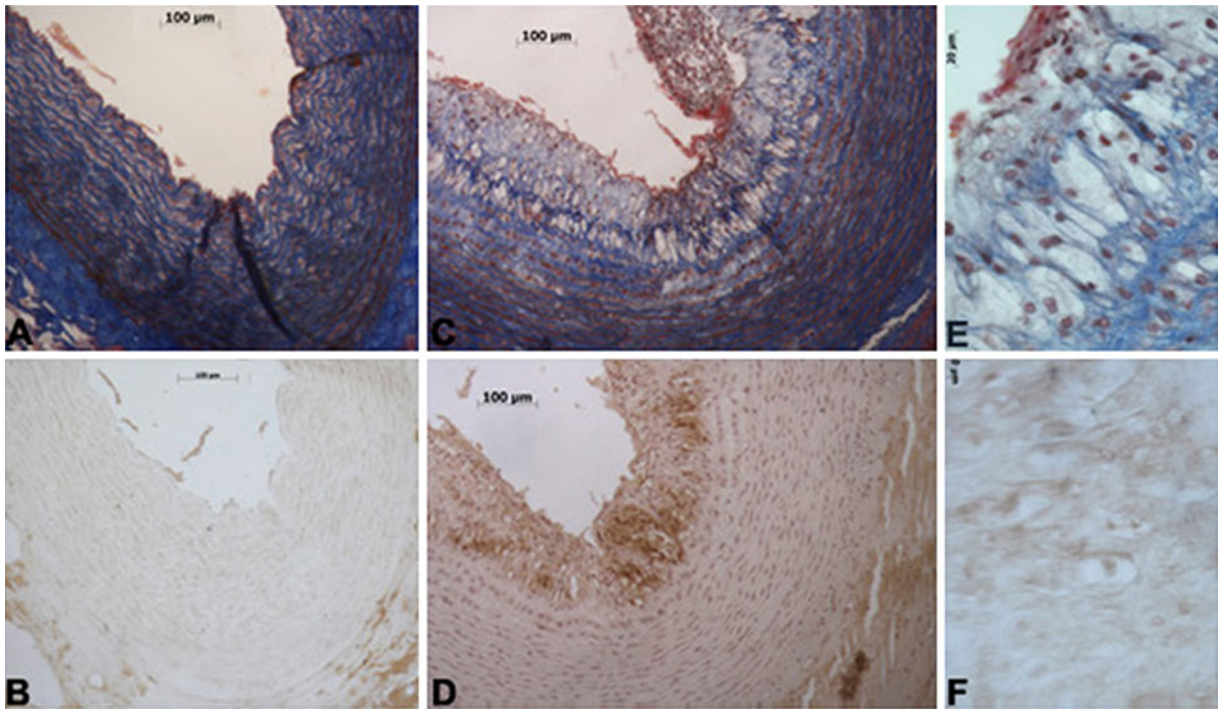

Fig. 1 Analysis of aortic arch from control and cholesterol-fed rabbits. Serial cross-sections showing immunohistochemical staining of aortic arch of rabbits fed either a normal diet or cholesterol diet. **a**, **c** Sections obtained from representative control or cholesterol-fed rabbit, respectively, stained with Azan Mallory's (original magnification, 10×). **b**, **d** Sections obtained from representative control or cholesterol-fed rabbit, respectively, stained with RAM11 monoclonal antibody (original magnification, 10×). **e**, **f** Particular of atherosclerotic lesion stained with Azan Mallory's method or RAM11 monoclonal antibody (original magnification, 40×). In **d** and **f**, positive immunostaining is indicated by a *brown color*

ApoA-I or ApoE were titrated by ELISA, using anti-ApoA-I or anti-ApoE antibodies, respectively. The level of ApoA-I progressively decreased in cholesterol-fed rabbits during treatment, as compared to that in controls (4 weeks, 30.3±1.4 vs. 44.2±1.7 μM, $P<0.01$; 8 weeks, 18.5±1.7 vs. 45±2.5 μM, $P<0.01$) (Fig. 4a). The level of ApoE was found markedly increased in cholesterol-fed rabbits (4 weeks, 16.1±1.4 vs. 2±0.2 μM in controls, $P<0.01$; 8 weeks, 30.5±2.9 vs. 1.3±0.5 μM, $P<0.01$) (Fig. 4b). The decrease in ApoA-I level concomitantly accompanied the increase in ApoE level from just the start of the treatment. A negative correlation was found between these levels ($r=-0.9462$, $P<0.01$), and the function which better described the changes of ApoE/ApoA-I during treatment was represented by a linear curve ($r=0.948$).

In order to measure the ApoE amount in HDL and non-HDL lipoproteins from cholesterol-fed rabbits, the plasma was collected after 8 weeks of treatment and processed by ELISA. Plasma aliquots were analyzed as such, and after fractionation with DS. ApoE was mostly (over 90 %) found as HDL-bound form (30.5±2.9 μM in HDL fraction), whereas in control animals, the amount of HDL-bound form was comparable to that in non-HDL fraction (Fig. 5). These findings indicate that cholesterol loading essentially caused ApoE accumulation in the HDL fraction. Conversely, ApoA-I levels in the HDL fraction and in the whole plasma were comparable both in control (45±2.5 and 47.4±1.9 μM, respectively) and cholesterol-fed rabbits (18.5±1.7 and 18.9±1.5 μM, respectively).

Effect of ApoE/ApoA-I ratio on LCAT activity in vitro

Proteoliposomes containing either ApoE or ApoA-I or different molar ratios of ApoE with ApoA-I (4:0, 3:1, 2:2, 1:3, or 0:4) were used to stimulate LCAT in vitro. Proteoliposomes with ApoE stimulated the enzyme 1.97-fold less than those with ApoA-I (4±0.12 vs. 7.86±0.04 U, $P<0.01$), and the enzyme activity decreased as the ApoE/ApoA-I ratio increased (Fig. 6a). These data indicate that LCAT activity is negatively

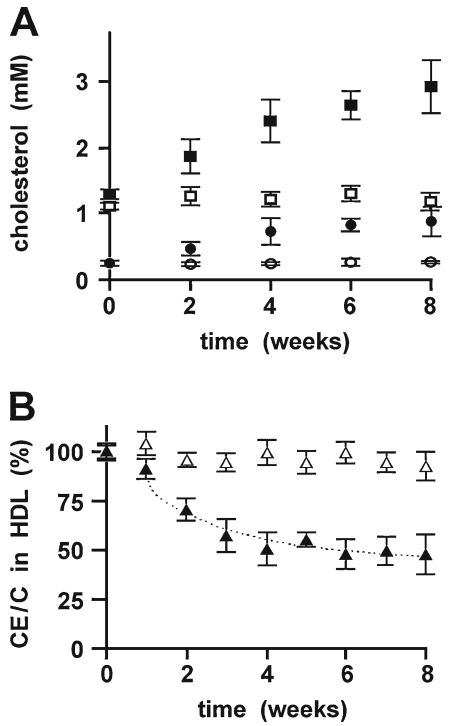

Fig. 2 FC and CE levels in HDL, from control and cholesterol-fed rabbits, at different times of treatment. The HDL fraction was isolated from plasma of cholesterol-fed or control rabbits, and analyzed for its FC and CE content by HPLC. **a** The concentrations of FC and CE in treated (*full circles* and *squares*, respectively) or control rabbits (*open circles* and *squares*, respectively) at 0, 2, 4, 6, and 8 weeks are shown. **b** The molar ratio of CE with FC in treated (N=5; *full triangles*) or control rabbits (N=5; *open triangles*), was calculated at each time, and expressed as percent of the initial value in each animal. Data are expressed as mean±SD at each time length. The *dotted curve* represents the trend expressed by CE/FC=91.7–22.3 Ln (time) (r=0.9522)

correlated to the ApoE/ApoA-I ratio in vitro (r=−0.993). This association might exist also in vivo. To support this hypothesis, HDL isolated from plasma of treated rabbits, collected at weekly intervals, were analyzed for their ApoE/ApoA-I and CE/FC ratios. As a matter of fact, the HDL CE/FC ratio was found decreased as the ApoE/ApoA-I ratio increased during the cholesterol diet (Fig. 6b). In particular, CE/FC was negatively correlated to Ln [ApoE/ApoA-I] (P<0.001).

Distribution of ApoA-I and ApoE among HDL subclasses

To evaluate how cholesterol diet affect ApoA-I and ApoE distribution over the different HDL subclasses,

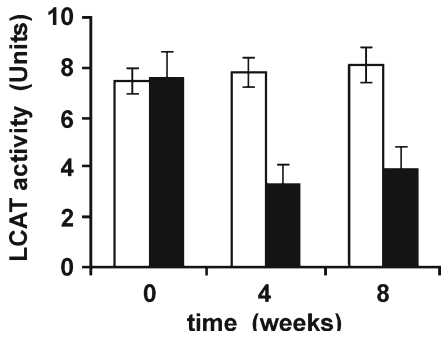

Fig. 3 Time-dependent modifications of LCAT activity in vitro. The in vitro activity of LCAT was measured in plasma samples from treated (N=5; *full bars*) and control rabbits (N=5; *open bars*), after 0, 4, and 8 weeks of treatment, using an ApoA-I-containing proteoliposome (0.7 μM) as substrate. The enzyme activity is expressed as enzyme units (nanomole of cholesterol esterified per hour per milliliter of sample). Data are reported as mean±SD at each time length

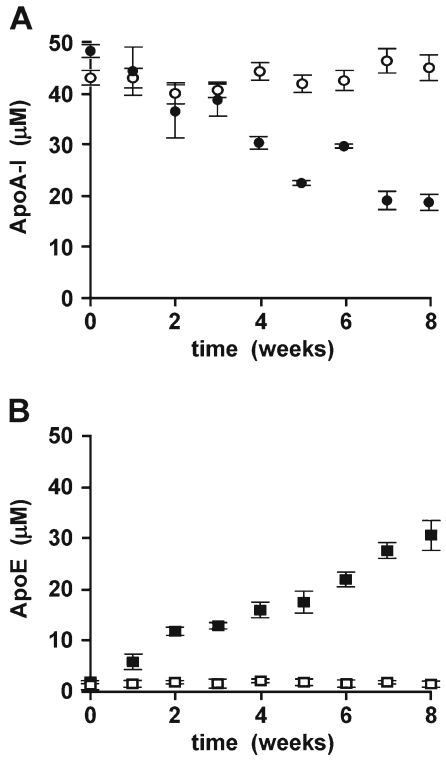

Fig. 4 Levels of ApoA-I and ApoE in normal and cholesterol treated rabbits. Plasma samples were collected from treated (N=5; *full symbols*) and control rabbits (N=5; *open symbols*) at different times (0, 2, 4, 6, and 8 weeks). The concentrations of ApoA-I (panel **a**) and ApoE (panel **b**) were measured by ELISA in samples of plasma, treated with 0.1 % DS and 50 mM $MnCl_2$ to remove VLDL and LDL. Data are expressed as mean±SD at each time length

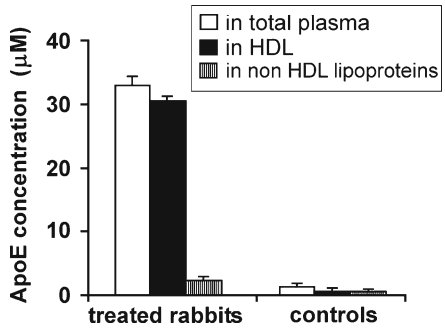

Fig. 5 ApoE level in plasma and lipoprotein fractions. Aliquots of plasma were collected, after 8 weeks of treatment, from both control (N=5) and treated (N=5) rabbits, and used as such or processed by DS for separating the HDL fraction from the non HDL fraction. The volumes of both fractions were adjusted to that of starting plasma. ApoE was titrated in the total plasma, in the HDL fraction, and in the non HDL lipopropotein fraction of each rabbit (see the *insert* for symbols). Each sample was analyzed in triplicate: deviations over 5 % from the average were not found. Data are expressed as mean±SD

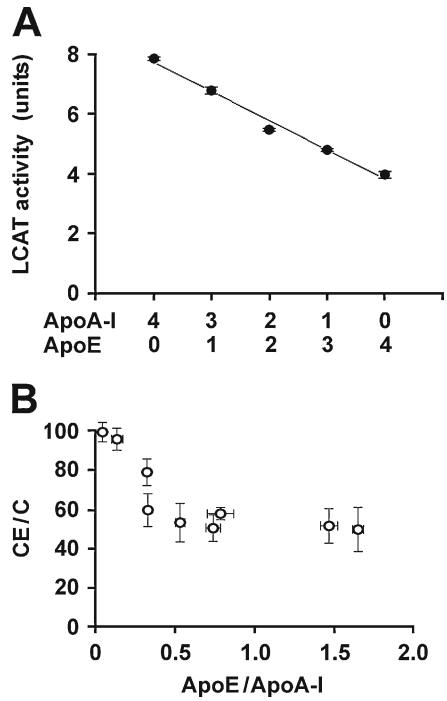

Fig. 6 Effect of ApoE/ApoA-I ratio on LCAT activity in vitro, and on CE/FC in HDL. **a** LCAT activity was analyzed in vitro by using a pool of DS-treated plasma, obtained from control rabbits, as enzyme source and liposomes containing ApoA-I, or ApoE, or different molar ratios of both apolipoproteins as substrate. The activity is expressed as enzyme units (nanomoles of cholesterol esterified per hour per milliliter of plasma). The data are reported as mean±SD. The negative correlation is graphically represented by the *drawn curve* (r=0.9928). **b** Correlation between CE/FC and ApoE/ApoA-I ratio. Plasma samples were collected at 1 week intervals during treatment of rabbits (N=5) with cholesterol-supplemented diet. Each sample was used to measure the molar concentration of ApoE, Apo A-I, FC, and CE in isolated HDL. The data are expressed as means±SD

the HDL fraction from cholesterol-fed rabbits was processed by non-denaturing electrophoresis and immunoblotting with antibodies against ApoA-I and ApoE (Fig. 7a). Three distinct patterns of immunoreactivity to antibodies against ApoA-I or ApoE were observed in HDL samples analyzed at different times of treatment (0, 4, and 8 weeks). Densitometric scanning of antibody-reacted ApoA-I or ApoE in the fractionated HDL population was carried out (Fig. 7). In samples collected at the beginning of treatment, HDL particles of 10.55 and 7.47 nm contained most of ApoA-I (40.3 % and 19 % of total amount, respectively). In samples collected after 4 weeks, the ApoA-I amount increased in the HDL particles sized from 7.6 to 9 nm, whereas it decreased in particles of 10.55 and 7.47 nm. After 8 weeks of treatment, ApoA-I decreased in all the HDL population, and was mostly associated to the HDL subclasses with 9 and 10.55 nm particle size.

ApoE was not detected in HDL isolated from plasma of cholesterol-fed rabbits at baseline (time 0). After 4 weeks of treatment, ApoE was present in large HDL particles (19.6 and 21.6 nm) and mostly associated to those displaying 19.6 nm size particles (73.6 % of the total amount). After 8 weeks, ApoE was mostly detected in 21.6 nm sized particles (63.2 % of the total amount). Furthermore, at this time, ApoE was detected in 9 and 10.55 nm sized particles (7.5 % and 13.7 % of the total amount, respectively).

Correlation of ApoE/ApoA-I or CE/FC with parameters of cardiovascular dysfunction

Previous studies investigated the relationship between structural and functional changes in the carotid arteries and LV myocardial function in patients with cardiovascular risk factors and found that LV relaxation is significantly associated with carotid stiffness [23]. Notably, ultrasonic strain imaging revealed subclinical changes in intrinsic myocardial deformation that could not be detected by the conventional methods, including transmitral flow and mitral annular motion velocities, used to evaluate LV function [23].

Although echocardiographic indices of cardiac function are different end-point from the functional

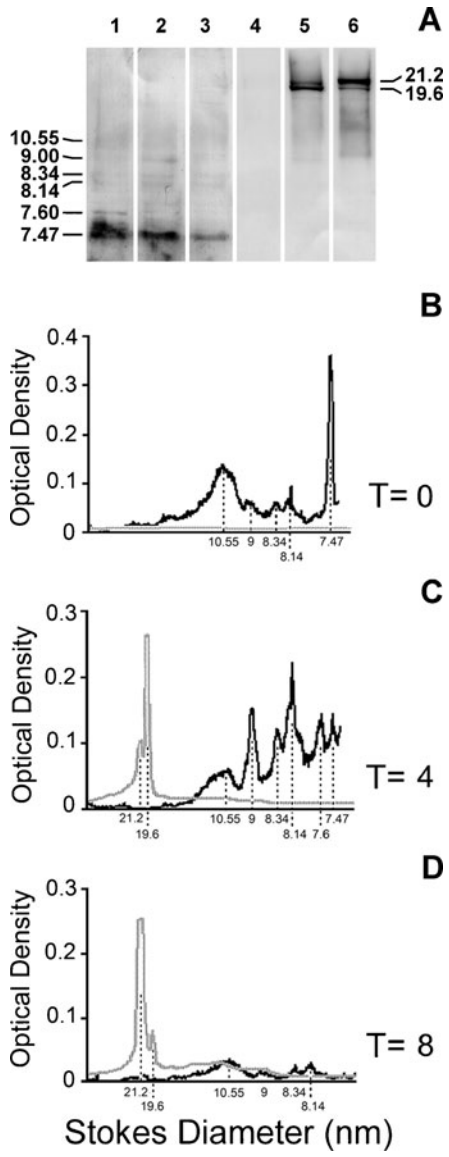

Fig. 7 Distribution of ApoA-I and ApoE among the HDL subclasses. Plasma samples from rabbits (N=5) were collected and pooled at time 0, and after 4 or 8 weeks of cholesterol diet. The HDL population was fractionated by electrophoresis on 4–30 % (*w*/*v*) polyacrylamide gradient gel, followed by immunostaining with anti-ApoA-I IgGs or Anti ApoE IgGs. **a** Representative Western Blot for ApoA-I (lanes *1*, *2*, and *3* represent 0, 4, and 8 weeks of cholesterol diet, respectively) and ApoE (*lanes 4*, *5*, and *6* represent 0, 4, 8 weeks of cholesterol diet, respectively). Numbers on both sides refer to Stokes' diameter values, calculated by using a calibration curve with globular proteins as migration standards. **b**–**d** The band intensities of ApoA-I and ApoE, detected at each time of treatment, were recorded as peaks on a densitogram, and arbitrarily expressed as Integrated Optical Density (IOD). The fractionation patterns of lipoproteins containing ApoA-I (*black*) or ApoE (*gray*) are shown. Particle sizes are expressed as Stokes' diameters. **b** Time 0; **c** 4 weeks of treatment; **d** 8 weeks of treatment

end-points we focused in our study, we also studied whether cardiac function indexes, as well as IMT, undergoes a variation during cholesterol loading, and whether this alteration is associated to changes of apolipoproteins or CE/FC ratio. All cardiac indices evaluated by echocardiography are reported in Table 1. Data obtained at the beginning of the treatment and after 4 or 8 weeks, indicate that IMT significantly increased whereas SR-s and S decreased during atherosclerosis progression in rabbit (Table 1). No change in these parameters was found in controls. In detail, the putative markers of atherosclerosis studied (HDL associated-ApoE/ApoA-I and CE/FC) were compared with IMT, a validated morphological marker of the disease, and with the cardiac function indexes SR-s and S, which reliably reflect myocardial contractility. In cholesterol-fed rabbits, IMT was positively correlated with SR-s and S (r=0.96, P<0.05 and r=0.96, P<0.05, respectively), and SR-s was positively correlated with S (r=0.96, P<0.05). The values of IMT were found positively correlated with ApoE (r=0.99, P<0.01) and negatively correlated with ApoA-I (r=0.99, P<0.01). SR-S and S positively correlated also with ApoE (r=0.98, P<0.05 and r=0.99, P<0.01, respectively) and negatively with ApoA-I (r=0.96, P<0.05 and r=1, P<0.01, respectively). The values of IMT, SR-s, and S were matched with those of the ApoE/ApoA-I ratio in homologous samples of plasma. This ratio was found positively correlated with IMT (r=0.99, P<0.01), and both SR-S (r=0.99, P<0.01) and Strain (r=0.95, P<0.05) (Fig. 8). No correlation between the CE/FC ratio and IMT, SR-S, or S was found. These results further suggest that, as atherosclerosis rises, the analysis of the levels of both ApoE and ApoA-I or the ApoE/ApoA-I ratio (an index of the changes in both proteins), might reflect the worsening of cardiovascular conditions whereas CE/FC, although representing an early response to cholesterol loading, does not mark the disease severity in later stages of treatment.

Discussion

Our results show that cholesterol diet induces in rabbit plasma an increase in ApoE concentration, and a

Table 1 Echocardiographic parameters and IMT measured in control and treated rabbits

Echocardiographic parameters	Sample	Time 0	Time 4 weeks	Time 8 weeks
Body weight (kg)	C	1.42±0.03	2.71±0.06*	3.44±0. 21*,**
	T	1.37±0.06	2.78±0.31*	3.31±0.38*, **
SIVd (mm)	C	2.02±0.15	2.00±0.08	1.95±0.06
	T	2.05±0.12	2.07±0.21	2.13±0.06
PPd (mm)	C	2.05±0.10	2.00±0.18	1.95±0.13
	T	2.06±0.08	2.08±0.28	2.03±0.11
LVd (mm)	C	15.35±0.85	15.35±0.85	15.12±0.58
	T	15.57±0.78	15.60±1.00	16.20±0.30
SIVs (mm)	C	3.02±0.26	3.01±0.28	3.05±0.24
	T	3.03±0.26	2.91±0.18	2.97±0.25
PPs (mm)	C	3.10±0.18	3.10±0.23	3.20±0.10
	T	3.12±0.17	3.13±0.18	3.17±0.25
LVs (mm)	C	10.60±0.96	10.50±0.96	10.60±0.64
	T	10.80±0.84	10.40±0.90	11.80±0.72
EF (%)	C	64.00±3.90	63.20±2.70	63.50±2.40
	T	63.00±3.50	64.60±3.30	64.70±3.10
SF (%)	C	34.00±4.10	33.70±3.80	34.20±3.10
	T	32.80±3.70	33.60±3.00	33.00±2.00
IMT (mm)	C	0.19±0.03	0.19±0.03	0.19±0.02
	T	0.19±0.01	0.21±0.01	0.23±0.03*
Strain (%)	C	−31.00±1.35	−31.25±1.25	−30.25±0.85
	T	−30.30±0.21	−26.50±0.56*	−23.30±0.88*, **
Strain rate S	C	−2.86±0.05	−2.85±0.03	−2.82±0.03
	T	−2.87±0.03	−2.49±0.22	−1.8±0.05*, **
Strain rate E	C	2.60±0.53	2.60±0.53	2.50±0.28
	T	2.65±0.48	2.50±0.48	2.65±0.11

The data are expressed as means±standard deviation. Statistical differences were calculated by one-way ANOVA followed by Tukey's test for multiple comparisons

*Significantly different from time 0 ($p<0.01$); **significantly different from 4 weeks ($p<0.05$)

C rabbit fed with normal diet, *T* rabbit fed with 2 % cholesterol-supplemented diet, *SIVd* end-diastole interventricular septum thickness, *PPd* end-diastole posterior wall thickness, *LVd* left ventricular diastolic diameter, *SIVs*, end-systole interventricular septum thickness, *PPs* end-systole posterior wall thickness, *LVs* left ventricular systolic diameter, *EF* ejection fraction, *SF* shortening fraction, *IMT* intima media thickness

decrease in both the LCAT activity and the level of ApoA-I, which is the LCAT major stimulator. This enzyme function can actually be limited or lost under inflammatory conditions [17]. The decrease of ApoA-I concentration in HDL, during atherogenesis, can depend on reduced synthesis, enhanced clearance, or replacement by serum amyloid A [17, 25]. Both human and animal studies showed that a high cholesterol diet leads to elevations in ApoE plasma levels [20, 22]. ApoE concentration also increased in patients with coronary artery disease [28]. Thus, CE depletion, ApoA-I decrease, and ApoE increase [17, 20, 22] in HDL are all resulting from traffic and activities on the scenario of altered RCT. The CE/FC molar ratio (rather than the concentration of either) in HDL might reflect the complex pathways of lipid metabolism in RCT and mark compositionally altered HDL. We actually found this ratio decreased during the first stages of treatment (0 to 4 weeks), as expected by the alteration of LCAT activity and the levels of its effectors. This enzyme was expected to work less than in normal conditions as atherosclerosis worsened, just because

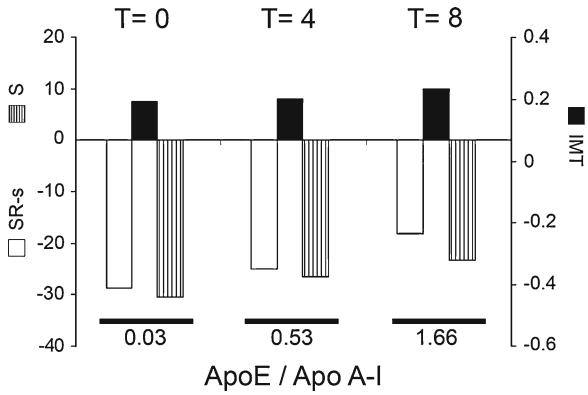

Fig. 8 Correlation between ApoE/ApoA-I ratio and IMT, SR-s, or S. Rabbits were analyzed at the beginning of treatment with cholesterol diet (t=0) and after 4 and 8 weeks (t=4 and t=8, respectively). Measurements of SR-s, S, and IMT were performed by image analysis for each animal, and the average is reported: deviations over 5 % from the average were not found. The ratio ApoE/ApoA-I in HDL was determined in triplicates from each sample, and the average values were used to obtain means±SD, as indicated on the figure bottom. This ratio is positively correlated with SR-s (P<0.01), S (P<0.05), and IMT (P<0.01)

the stimulation on the enzyme activity decreased. In fact, the increase of ApoE level during the treatment could not make up for the decrease of ApoA-I level. In vitro LCAT stimulation by ApoE was actually found to be about a half of that by ApoA-I, according to previous information [42]. We also report here experimental evidence that ApoE liposomes stimulated rabbit LCAT less efficiently than ApoA-I liposomes. However, since it has been reported that ApoE is more efficient than ApoA-I as LCAT activator on large HDL particles [42], it cannot be excluded that the constant trend of the ratio CE/FC, at late stages of treatment, could be due to the increase in ApoE concentration. Several lines of evidence suggested a potent anti-atherogenic role for ApoE. Indeed, ApoE −/− mice are severely hypercholesterolemic and rapidly develop atherosclerosis [37]. ApoE was reported to prevent the progression of atherosclerosis in hyperlipidemic rabbits [39]. A prominent HDL subclass, enriched in ApoE and referred to as HDL-1, was detected in cholesterol-fed rabbits [21]. We cannot exclude that ApoE might influence the rate of atherogenesis not only by modulating the RCT pathway but also by positively modifying cellular functions in the arterial wall.

LCAT activity might also be reduced by oxidative stress as it has been reported that oxidation of ApoA-I or ApoE, as occurring during inflammatory conditions, can be associated to the loss of the ability of these apolipoproteins to stimulate LCAT [29, 30]. It was recently shown that HDL from patients with coronary artery disease is oxidatively modified and that oxidation impairs RCT mediated by HDL [2, 24]. However cholesterol esterification, though negatively affected by reduced stimulation and possible oxidative stress, seems to be driven by enhanced levels of circulating cholesterol. Therefore, the observed poor change of CE/FC in HDL, during the second month of cholesterol-loading, might depend on balance between high CE production and increased availability of dietary cholesterol. Increased cholesterol availability might be also enhanced by reduced uptake by hepatocytes or macrophages. In fact, the expression of SR-BI was previously found significantly decreased in the liver of hypercholesterolemic rabbits as compared with control group [15, 41].

The HDL population shows considerable compositional heterogeneity with respect to both lipid and apolipoprotein components. As changes in these components among HDL subclasses might influence RCT and predict cardiovascular disease [35], we choose to analyze the distribution of ApoE and ApoA-I among HDL subclasses. Our analysis of the HDL population in the plasma of rabbits shows that cholesterol-diet, in the early stages of treatment, raises the amount of HDL-2, which are considered less efficient than HDL-3 in stimulating RCT and weakening atherosclerosis. In later stages of treatment, most of ApoE was localized in large HDL-1. This marked increase of ApoE concentration on HDL might represent a physiological response to face high cholesterol accumulation and counteract inflammation and atherosclerosis.

Previous studies showed that HDL and ApoA-I negatively correlated with IMT in humans [16]. Lower level of ApoA-I, higher level of ApoB, and the ratio ApoB/ApoA-I were suggested to be independent risk factors for coronary heart disease [26]. In addition, a link between ApoE phenotype prevalence and IMT was found [38]. S and SR reflect myocardial deformation properties [9, 33], do not depend on overall heart motion or rotation induced by contraction of adjacent myocardial segments, and reliably represent the heart local deformation [7, 36]. In particular, regional SR was proposed to be a strong index of left ventricular contractility [12]. Our study suggests that the analysis of S and SR-s, which was previously shown to be effective in detecting early subclinical myocardial abnormalities [9], allows detecting longitudinal myocardial damage

in rabbit treated with cholesterol diet. To our knowledge, this is the first time that SR-s imaging was used to compare right ventricular and left ventricular regional function in cholesterol-fed rabbit. The CE/FC ratio was not correlated with IMT or with the indices of cardiac function. On the other hand, we found the ratio ApoE/ApoA-I correlated both with IMT and with function S and SR-s. These data suggest that the alteration of ApoE/ApoA-I ratio, in HDL, might reflect the severity of atherosclerosis, as quantified by IMT, as well as the alteration of cardiac function, as evaluated by the cardiac parameters used in this study. This ratio might also reflect the HDL remodeling caused by the changes in enzyme activities and apolipoprotein metabolism occurring in response to high levels of dietary or endogenous cholesterol. In conclusion, our study suggests that the cardiac function might be altered by the increase of IMT, which in turn should be altered by changes in reverse cholesterol transport. Prospective studies on patients with atherosclerosis are required to verify whether relationships of cause–effect between insufficient RCT and cardiac function do exist and to confirm the usefulness of the ApoE/ApoA-I ratio as a marker for evaluating atherosclerosis progression in longitudinal analysis.

Acknowledgments This research was supported by a grant from the Ministry of Health of Italy (Project BS 1.2.5; upb 2.1.2.1, cap 2306). We thank Dr. Daniele Di Napoli for rabbits' treatment and Dr. Domenico Iossa for assistance in ELISA experiments.

References

1. Bachorik PS, Ross JW (1995) National Cholesterol Education Program recommendations for measurement of low-density lipoprotein cholesterol: executive summary. The National Cholesterol Education Program Working Group on Lipoprotein Measurement. Clin Chem 41:1414–1420
2. Bergt C, Pennathur S, Fu X et al (2004) The myeloperoxidase product hypochlorous acid oxidizes HDL in the human artery wall and impairs ABCA1-dependent cholesterol transport. Proc Natl Acad Sci USA 101:13032–13037
3. Brewer HB Jr, Ronan R, Meng M, Bishop C (1986) Isolation and characterization of apolipoproteins A-I, A-II, and A-IV. Methods Enzymol 128:223–246
4. Chen CH, Albers JJ (1985) Activation of lecithin: cholesterol acyltransferase by apolipoproteins E-2, E-3, and A-IV isolated from human plasma. Biochim Biophys Acta 836:279–285
5. Cigliano L, Pugliese CR, Spagnuolo MS et al (2009) Haptoglobin binds the antiatherogenic protein apolipoprotein E-impairment of apolipoprotein E stimulation of both lecithin: cholesterol acyltransferase activity and cholesterol uptake by hepatocytes. FEBS J 276:6158–6171
6. Cigliano L, Spagnuolo MS, Cuomo G et al (2005) Apolipoprotein A-I-dependent cholesterol esterification in patients with rheumatoid arthritis. Life Sci 7:108–120
7. D'Hooge J, Heimdal A, Jamal F et al (2000) Regional strain and strain rate measurements by cardiac ultrasound: principles, implementation and limitations. Eur J Echocardiogr 1:154–170
8. Desai MY, Rodriguez A, Wasserman BA et al (2005) Association of cholesterol subfractions and carotid lipid core measured by MRI. Arterioscler Thromb Vasc Biol 25:e110–e111
9. Di Salvo G, Drago M, Pacileo G et al (2005) Comparison of strain rate imaging for quantitative evaluation of regional left and right ventricular function after surgical versus percutaneous closure of atrial septal defect. Am J Cardiol 96:299–302
10. Forte A, Di Micco G, Galderisi U et al (2001) Molecular analysis of arterial stenosis in rat carotids. J Cell Physiol 186:307–313
11. Glomset JA, Janssen ET, Kennedy R, Dobbins J (1996) Role of plasma lecithin:cholesterol acyltransferase in the metabolism of high density lipoproteins. J Lipid Res 7:638–648
12. Greenberg NL, Firstenberg MS, Castro PL et al (2002) Doppler-derived myocardial systolic strain rate is a strong index of left ventricular contractility. Circulation 105:99–105
13. Greenow K, Pearce N, Ramji DP (2005) The key role of apolipoprotein E in atherosclerosis. J Mol Med 83:329–342
14. Hoeg JM, Santamarina-Fojo S, Bérard AM et al (1996) Overexpression of lecithin:cholesterol acyltransferase in transgenic rabbits prevents diet-induced atherosclerosis. Proc Natl Acad Sci U S A 93:11448–11453
15. Hong SC, Zhao SP, Wu ZH (2007) Effect of probucol on HDL metabolism and class B type I scavenger receptor (SR-BI) expression in the liver of hypercholesterolemic rabbits. Int J Cardiol 115:29–35
16. Juonala M, Viikari JSA, Kahonen M et al (2008) Childhood levels of serum apolipoproteins B and A-I predict carotid intima-media thickness and brachial endothelial function in adulthood. J Am Coll Cardiol 52:293–299
17. Kontush A, Chapman MJ (2006) Functionally defective high-density lipoprotein: a new therapeutic target at the crossroads of dyslipidemia, inflammation, and atherosclerosis. Pharmacol Rev 58:342–374
18. Li Z, McNamara JR, Ordovas JM, Schaefer EJ (1994) Analysis of high density lipoproteins by a modified gradient gel electrophoresis method. J Lipid Res 35:1698–1711
19. Lund-Katz S, Phillips MC (2010) High density lipoprotein structure-function and role in reverse cholesterol transport. Subcell Biochem 51:183–227
20. Mahley RW (1982) Atherogenic hyperlipoproteinemia. The cellular and molecular biology of plasma lipoproteins altered by dietary fat and cholesterol. Med Clin North Am 66:375–402
21. Mahley RW, Huang Y, Weisgraber KH (2006) Putting cholesterol in its place: apo E and reverse cholesterol transport. J Clin Invest 116:1226–1129

22. Mezdour H, Nomura S, Yamamura T, Yamamoto A (1992) Concentration and distribution of apolipoproteins A-I and E in normolipidemic, WHHL and diet-induced hyperlipidemic rabbit sera. Biochim Biophys Acta 1127:116–123
23. Mizuguchi Y, Oishi Y, Tanaka H et al (2007) Arterial stiffness is associated with left ventricular diastolic function in patients with cardiovascular risk factors: early detection with the use of cardio-ankle vascular index and ultrasonic strain imaging. J Card Fail 13:744–751
24. Pennathur S, Bergt C, Shao B et al (2004) Human atherosclerotic intima and blood of patients with established coronary artery disease contain high density lipoprotein damaged by reactive nitrogen species. J Biol Chem 279:42977–42983
25. Rashid S, Patterson BW, Lewis GF (2006) What have we learned about HDL metabolism from kinetics studies in humans? J Lipid Res 47:1631–1642
26. Rasouli M, Kiasari AM, Mokhberi V (2006) The ratio of apoB/apoAI, apoB and lipoprotein(a) are the best predictors of stable coronary artery disease. Clin Chem Lab Med 44:1015–1021
27. Rosenson RS, Otvos JD, Freedman DS (2002) Relations of lipoprotein subclass levels and low-density lipoprotein size to progression of coronary artery disease in the Pravastatin Limitation of Atherosclerosis in the Coronary Arteries (PLAC-I) trial. Am J Cardiol 90:89–94
28. Sacks FM, Alaupovic P, Moye LA et al (2000) VLDL, apolipoproteins B, CIII, and E, and risk of recurrent coronary events in the Cholesterol and Recurrent Events (CARE) trial. Circulation 102:1886–1892
29. Salvatore A, Cigliano L, Bucci EM et al (2007) Haptoglobin binding to apolipoprotein A-I prevents damage from hydroxyl radicals on its stimulatory activity of the enzyme lecithin-cholesterol acyl-transferase. Biochemistry 46:11158–11168
30. Salvatore A, Cigliano L, Carlucci A et al (2009) Haptoglobin binds apolipoprotein E and influences cholesterol esterification in the cerebrospinal fluid. J Neurochem 110:255–263
31. Schiller NB, Shah PM, Crawford M et al (1989) American Society of Echocardiography Committee on Standards. Recommendations for quantitation of the left ventricle by two-dimensional echocardiography. J Am Soc Echocardiogr 2:358–367
32. Spagnuolo MS, Cigliano L, D'Andrea LD et al (2005) Assignment of the binding site for Haptoglobin on Apolipoprotein A-I. J Biol Chem 280:1193–1198
33. Sutherland GR, Di Salvo G, Claus P et al (2004) Strain and strain rate imaging: a new clinical approach to quantifying regional myocardial function. J Am Soc Echocardiogr 17:788–802
34. Teichholz LE, Kreulen T, Herman MV, Gorlin R (1976) Problems in Echocardiographic volume determinations: Echocardiographic-angiographic correlations in the presence of asynergy. Am J Cardiol 37:7–11
35. Tian L, Fu M (2010) The relationship between high density lipoprotein subclass profile and plasma lipids concentrations. Lipids Health Dis 9:118–126
36. Urheim S, Edvardsen T, Torp H et al (2000) Myocardial strain by Doppler echocardiography validation of a new method to quantify regional myocardial function. Circulation 102:1158–1164
37. Véniant MM, Withycombe S, Young SG (2001) Lipoprotein size and atherosclerosis susceptibility in Apoe−/− and Ldlr−/− mice. Arterioscler Thromb Vasc Biol 21:1567–1570
38. Wohlin M, Sundstrom J, Lannfelt L et al (2007) Apolipoprotein E epsilon4 genotype is independently associated with increased intima-media thickness in a recessive pattern. Lipids 42:451–456
39. Yamada N, Inoue I, Kawamura M et al (1992) Apolipoprotein E prevents the progression of atherosclerosis in Watanabe heritable hyperlipidemic rabbits. J Clin Invest 89:706–711
40. Yanni AE (2004) The laboratory rabbit: an animal model of atherosclerosis research. Lab Anim 38:246–256
41. Zhao SP, Wu ZH, Hong SC et al (2006) Effect of atorvastatin on SR-BI expression and HDL-induced cholesterol efflux in adipocytes of hypercholesterolemic rabbits. Clin Chim Acta 365:119–124
42. Zorich N, Jonas A, Pownall HJ (1985) Activation of lecithin cholesterol Acyltransferase by human apolipoprotein E in discoidal complexes with lipids. J Biol Chem 260:8831–8837